Vol. **114** (2008) *ACTA PHYSICA POLONICA A* No. 5

Proc. XXXVII International School of Semiconducting Compounds, Jaszowiec 2008

Second-Order Resonant Polaron in a Self-Assembled Quantum Dot

P. Kaczmarkiewicz and P. Machnikowski

Institute of Physics, Wrocław University of Technology
Wybrzeże Wyspiańskiego 27, 50-370 Wrocław, Poland

We calculate numerically the spectrum of a polaron in a quantum dot in the region of resonance with two-phonon states. We show that the experimental data can be reproduced by a model that does not depend on any adjustable parameters.

PACS numbers: 73.21.La, 78.67.Hc, 71.38.−k, 63.20.kd

1. Introduction

A compound system consisting of an electron in a quantum dot (QD) and longitudinal optical (LO) phonons has interesting features that cannot be observed in higher-dimensional semiconductor structures. Because of a relatively large size of the QD (compared to the lattice constant), only long wavelength phonon modes are coupled to the electron. Since the LO phonons are almost dispersionless in the vicinity of the Γ point, these effectively coupled modes can be represented as a system of discrete oscillators, rather than a continuum. As a result of the interaction between the confined electron and the set of LO phonon oscillators with a well-defined frequency, pronounced anticrossings are observed in the intraband absorption spectra of a single dot whenever the energy difference between electron levels matches a multiple of the LO phonon energy [1].

Such resonant polarons are an object of current interest, both from the point of view of their properties in various QD systems as well as of the formal methods that can be used to describe them [2–4]. The spectrum of a resonant polaron can easily be described for a single-phonon (first order) resonance [5]. However, in most self-assembled structures the energy spacing between the electron levels considerably exceeds the LO phonon energy. In fact, resonances observed in experiments performed at moderate magnetic fields occur at the crossing of the electron levels with *twice* the LO phonon energy. Contrary to the first-order resonance, modeling of two-phonon polaron states is less trivial, since the carrier–phonon interaction has no matrix elements directly coupling the anticrossing states. Thus, the effect

is of second order but must be treated non-perturbatively in order to reproduce the strong-coupling behavior at the resonance.

In this paper, we study the spectrum of a confined polaron, that is, an electron–LO phonon system in a self-assembled InAs/GaAs QD coupled by the Fröhlich interaction. We focus on the second-order resonance between the ground state with two phonons and the first electronic shell, composed of the states with the angular momentum along the QD symmetry axis equal to $m = \pm 1$. As in the experiment [1], the states are brought to resonance by the Zeeman shift of the $m = -1$ line.

2. The model

The system is described by the Hamiltonian

$$H = H_0 + H_{\rm a} + H_{\rm int} + H_{\rm ph}, \tag{1}$$

where H_0 describes an electron in an isotropic dot, $H_{\rm a}$ accounts for the QD anisotropy, $H_{\rm int}$ describes the electron–phonon coupling and $H_{\rm ph}$ is the free LO phonon Hamiltonian.

The first term in Eq. (1) is the Fock–Darwin Hamiltonian [6] describing an electron in an isotropic, 2-dimensional harmonic potential in the QD plane (xy) with an eigenfrequency ω_0, in a perpendicular magnetic field. The dynamics along the strongly confined z direction is restricted to the lowest subband. For the calculations of electron–phonon coupling constants we will assume a Gaussian envelope wave function in this direction with the width l_z. Throughout this paper we will use the basis of eigenfunctions of this Hamiltonian, denoted as $|nm\rangle$, where $n = 0, 1, \ldots$ and $m = \ldots, -1, 0, 1, \ldots$ are the radial and angular momentum quantum numbers of the corresponding Fock–Darwin state [6], respectively (that is, $\hbar m$ is the projection of the angular momentum on the symmetry axis z). In this basis the Hamiltonian is

$$H_0 = \sum_{nm} \epsilon_{nm} |nm\rangle\langle nm|, \qquad \epsilon_{nm} = \hbar\omega_{\rm B}(2n + |m| + 1) - \frac{1}{2}\hbar\omega_{\rm c} m,$$

with $\omega_{\rm B}^2 = \omega_0^2 + \omega_{\rm c}^2/4$, where $\omega_{\rm c} = eB/m^*$ is the cyclotron frequency in the magnetic field B and $m^* = 0.066 m_{\rm e}$ is the effective mass of an electron in GaAs.

The second term describes a weak anisotropy (ellipticity) of the confinement potential and has the form

$$H_{\rm a} = \frac{\beta}{2} m^* \omega_0^2 (x^2 - y^2) = \frac{\beta}{2} \frac{\hbar\omega_0^2}{\omega_{\rm B}} \sum_{nm,n'm'} V_{(nm)(n'm')} |nm\rangle\langle n'm'|,$$

where β is a parameter and the matrix elements in the basis of Fock–Darwin states are

$$V_{(0\bar{2})(00)} = V_{(00)(0\bar{2})} = V_{(02)(00)} = V_{(00)(02)} = \frac{\sqrt{2}}{2},$$

$$V_{(0\bar{2})(10)} = V_{(10)(0\bar{2})} = V_{(02)(10)} = V_{(10)(02)} = \sqrt{2},$$

$$V_{(0\bar{1})(01)} = V_{(01)(0\bar{1})} = 1.$$

Here and throughout the paper a bar over a number denotes a minus sign.

The electron–phonon coupling Hamiltonian has the form [5]:

$$H_{\rm int} = \sum_{nmn'm'} |nm\rangle\langle n'm'| \sum_{\boldsymbol{k}} F_{(nm)(n'm')}(\boldsymbol{k}) b_{\boldsymbol{k}} + \text{h.c.},$$

where

$$F_{(nm)(n'm')}(\boldsymbol{k}) = \sqrt{\frac{\hbar\Omega}{2V\varepsilon_0\tilde{\varepsilon}}}\frac{e}{k} f_{(nm)(n'm')}\left(\frac{l_{\rm B}k_\perp}{2}\right) \mathrm{e}^{-(l_{\rm B}k_\perp/2)^2-(l_z k_z/2)^2} \times \mathrm{e}^{\mathrm{i}(m'-m)\phi}.$$

Here the wave vector is written as $\boldsymbol{k} = (k_\perp\cos\phi, k_\perp\sin\phi, k_z)$, Ω is the frequency of LO phonons at $\boldsymbol{k} = 0$, V is the normalization volume for the phonon modes, ε_0 is the vacuum permeability, $\tilde{\varepsilon}$ is the low-frequency part of the dielectric constant, and $l_{\rm B} = \sqrt{\hbar/(m\omega_{\rm B})}$ is the confinement width in the magnetic field. Let us note that the Gaussian cut-off at $k \sim 1/l_{\rm B}$ restricts the coupling only to long-wavelength modes, so the frequency of LO phonons can be replaced by its value at the center of the Brillouin zone. The functions $f_{(nm)(n'm')}(q)$ are tabulated in Table I.

The last contribution to the Hamiltonian is $H_{\rm ph} = \hbar\Omega\sum_{\boldsymbol{k}} b^\dagger_{\boldsymbol{k}} b_{\boldsymbol{k}}$.

TABLE I

Functions $f_{(nm)(n'm')}(q)$ used in the definition of coupling constants.

nm	00	01	10	02
00	1	$-\mathrm{i}q$	$-q^2$	$-q^2/\sqrt{2}$
$0\bar{1}$	$-\mathrm{i}q$	$-q^2$	$\mathrm{i}(q^3-q)$	$\mathrm{i}q^3/\sqrt{2}$
01	$-\mathrm{i}q$	$1-q^2$	$\mathrm{i}(q^3-q)$	$\mathrm{i}(q^3-2q)/\sqrt{2}$
10	$-q^2$	$\mathrm{i}(q^3-q)$	$1-2q^2+k^4$	$(q^4-2q^2)/\sqrt{2}$
$0\bar{2}$	$-q^2/\sqrt{2}$	$\mathrm{i}q^3/\sqrt{2}$	$(q^4-2q^2)/\sqrt{2}$	$q^4/2$
02	$-q^2/\sqrt{2}$	$\mathrm{i}(q^3-2q)/\sqrt{2}$	$(q^4-2q^2)/\sqrt{2}$	$1-2q^2+q^4/2$

3. The method

Our approach to the diagonalization of the Hamiltonian (1) is based on the collective mode representation of the LO phonons [7]. The basis of the electron subsystem is composed of up to 6 lowest Fock–Darwin states (3 lowest energy shells, $2n+|m|+1 \le 3$). For this truncated basis, we define 14 collective phonon modes which are needed to exactly represent the carrier–phonon coupling,

$$B_{M\alpha} = \sqrt{\frac{l_{\rm B}}{V}}\sum_k \frac{1}{k}\phi_{M\alpha}\left(\frac{l_{\rm B}k_\perp}{2}\right)\mathrm{e}^{(l_{\rm B}k_\perp/2)^2-(l_z k_z/2)^2}\mathrm{e}^{\mathrm{i}M\phi},$$

where $\alpha = A, B, C$ labels different modes with the same angular momentum M

TABLE II

Functions $\phi_{M\alpha}(q)$ used in the definition of collective modes. The numbers x_l are defined as $x_l = (4\pi^3)^{-1}\int \mathrm{d}^3q q_\perp^l \exp\left(-2(q_\perp^2+q_z^2\lambda^2)\right)/q^2$, where $\lambda = l_z/l_\mathrm{B}$. We defined also $a_2 = \frac{x_2x_4x_8-x_4^2x_6}{\sqrt{x_4^2x_8-x_4x_6^2}}$, $a_4 = \frac{x_2x_4x_6-x_4^3}{\sqrt{x_4^2x_8-x_4x_6^2}}$ and $c = x_0 - 2a_2x_2 + 2a_4x_4 + a_2^2x_4 - 2a_2a_4x_6 + a_4^2x_6$.

	$\alpha = A$	$\alpha = B$	$\alpha = C$
$M = 0$	$-q^2/\sqrt{x_4}$	$\frac{x_4q^4-x_6q^2}{\sqrt{x_4^2x_8-x_4x_6^2}}$	$(1-a_2q^2+a_4q^4)/\sqrt{c}$
$M = \pm1$	$\mathrm{i}q/\sqrt{x_2}$	$\frac{\mathrm{i}(x_2q^3-x_4q)}{\sqrt{x_6x_2^2-x_4^2x_2}}$	
$M = \pm2$	$-q^2/\sqrt{x_4}$	$\frac{x_4q^4-x_6q^2}{\sqrt{x_4^2x_8-x_4x_6^2}}$	
$M = \pm3$	$\mathrm{i}q^3/\sqrt{x_6}$		
$M = \pm4$	$q^4/\sqrt{x_8}$		

TABLE III

Coupling constants $\gamma_{(nm)(n'm')}$ for the collective LO modes. Definitions as in Table II. Omitted coupling constants can be found from the relation $\gamma_{(n\bar{m})(n'\bar{m}')\alpha} = \gamma_{(nm)(n'm')\alpha}$.

nm	00	01	10	02
$00A$	$\frac{a_4x_6}{\sqrt{x_4}} - a_2\sqrt{x_4}$	$-\sqrt{x_2}$	$\sqrt{x_4}$	$\sqrt{x_4/2}$
B	$-a_4\sqrt{x_8-\frac{x_6^2}{x_4}}$			
$0\bar{1}A$	$-\sqrt{x_2}$	$\sqrt{x_4}$	$\frac{x_4}{\sqrt{x_2}} - \sqrt{x_2}$	$\sqrt{x_6/2}$
B			$\sqrt{x_6-\frac{x_4^2}{x_2}}$	
$01A$	$-\sqrt{x_2}$	$\frac{a_4x_6-a_2x_4+x_4}{\sqrt{x_4}}$	$\frac{x_4}{\sqrt{x_2}} - \sqrt{x_2}$	$\frac{x_4}{\sqrt{2x_2}} - \sqrt{2x_2}$
B		$-a_4\sqrt{x_8-\frac{x_6^2}{x_4}}$	$\sqrt{x_6-\frac{x_4^2}{x_2}}$	$\sqrt{\frac{x_6}{2}-\frac{x_4^2}{2x_2}}$
$10A$	$\sqrt{x_4}$	$\frac{x_4}{\sqrt{x_2}} - \sqrt{x_2}$	$\frac{2x_4-a_2x_4+x_6a_4-x_6}{\sqrt{x_4}}$	$\sqrt{2x_4} - \frac{x_6}{\sqrt{2x_4}}$
B		$\sqrt{x_6-\frac{x_4^2}{x_2}}$		$\sqrt{\frac{x_8}{2}-\frac{x_6^2}{2x_4}}$
$0\bar{2}A$	$\sqrt{x_4/2}$	$\sqrt{2x_4} - \frac{x_6}{\sqrt{2x_4}}$	$\sqrt{2x_4} - \frac{x_6}{\sqrt{2x_4}}$	$\sqrt{x_8}/2$
B		$\sqrt{\frac{x_8}{2}-\frac{x_6^2}{2x_4}}$	$\sqrt{\frac{x_8}{2}-\frac{x_6^2}{2x_4}}$	
$02A$	$\sqrt{x_4/2}$	$\frac{x_4}{\sqrt{2x_2}} - \sqrt{2x_2}$	$\sqrt{2x_4} - \frac{x_6}{\sqrt{2x_4}}$	$\sqrt{x_4}(2-a_2+\frac{x_6a_4}{x_4}-\frac{x_6}{2x_4})$
B		$\sqrt{\frac{x_6}{2}-\frac{x_4^2}{2x_2}}$	$\sqrt{\frac{x_8}{2}-\frac{x_6^2}{2x_4}}$	

and the functions $\varphi_{M\alpha}(q)$ are listed in Table II. With this definition the collective operators $B_{M\alpha}, B_{M\alpha}^\dagger$ satisfy the usual bosonic commutation relations, $[B_{M\alpha}, B_{M'\alpha'}^\dagger] = \delta_{MM'}\delta_{\alpha\alpha'}$. In terms of the collective modes, the interaction Hamiltonian reads

$$H_{\rm int} = \sum_{nmn'm'} \sum_{\alpha} |nm\rangle\langle n'm'|\gamma_{(nm)(n'm')\alpha} B_{m'-m,\alpha} + \text{h.c.}, \tag{2}$$

where the coupling constants $\gamma_{(nm)(n'm')\alpha}$ are collected in Table III. The Hamiltonian (2) is then diagonalized numerically, including states with up to 3 phonons, which yields a computational basis of 4080 states.

4. Results

The result of the numerical diagonalization is shown in Fig. 1a. The figure shows the states that have large overlap with purely electronic (i.e., zero-phonon) basis states. Qualitatively, the spectral branches reproduce the experimental results obtained from far infrared absorption on a single QD [1]. A sensitive quantitative benchmark for the accuracy of the modeling is the width of the resonance δE and, to a smaller extent, its position B_0 (which, however, is not precisely defined by the experimental results due to almost parallel branches and some degree of noise in the anticrossing region). The values read off the experimental results [1] are $\delta E = 2.9$ meV and B_0 in the range 12–14 T. Our numerical results reproduce these two values very well.

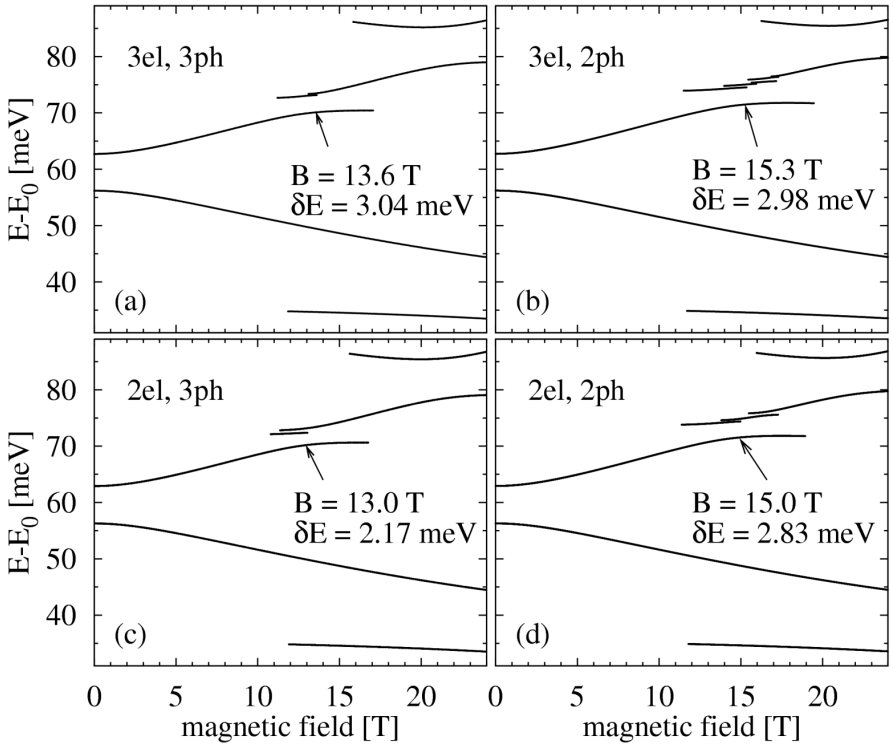

Fig. 1. The results of the numerical diagonalization of the electron–phonon Hamiltonian using different computational bases ("el": number of the Fock–Darwin shells, "ph": maximum number of phonons). The position and width of the resonance are indicated.

For comparison, in Figs. 1b–d we plot the results obtained from reduced models, with lower number of electron energy shells and/or lower maximum number of LO phonons. Although the curves obtained from reduced models may look similar to those obtained from the full model, they differ (even qualitatively) from the latter in the resonance area. In all three cases, artifact lines, slightly split off the upper branch, appear in this range of magnetic fields. Also quantitatively, the agreement with the experiment is lost: reducing the number of phonons shifts the resonance to higher magnetic fields (Fig. 1b,d), while the model with up to 3 phonons but only 2 electronic shells (Fig. 1c) yields a strongly underestimated resonance width.

5. Conclusions

We have found the spectrum of a second-order polaron formed by a p-shell state of an electron confined in a quantum dot coupled to two-phonon states. Our parameter-free model reproduces the observed values of the resonance position and width without any need to adjust material constants, contrary to what was originally suggested [1].

We have studied also the effects of restricting the computational basis. It turns out that the model used in our computations is minimal in the sense that further truncation of the number of electron or phonon states leads to qualitative and quantitative discrepancies as compared to both the full model and the experimental data. The achieved correct modelling of the resonant polaron states opens the way to a quantitative description of polaron relaxation, which continues to be an open issue both in theoretical and experimental investigations.

References

[1] S. Hameau, Y. Guldner, O. Verzelen, R. Ferreira, G. Bastard, J. Zeman, A. Lemaître, J.M. Gerard, *Phys. Rev. Lett.* **83**, 4152 (1999).

[2] O. Verzelen, R. Ferreira, G. Bastard, *Phys. Rev. Lett.* **88**, 146803 (2002).

[3] T. Stauber, R. Zimmermann, *Phys. Rev. B* **73**, 115303 (2006).

[4] D. Obreschkow, F. Michelini, S. Dalessi, E. Kapon, M.-A. Dupertuis, *Phys. Rev. B* **76**, 035329 (2007).

[5] L. Jacak, J. Krasnyj, D. Jacak, P. Machnikowski, *Phys. Rev. B* **67**, 035303 (2003).

[6] L. Jacak, P. Hawrylak, A. Wojs, *Quantum Dots*, Springer Verlag, Berlin 1998.

[7] T. Stauber, R. Zimmermann, H. Castella, *Phys. Rev. B* **62**, 7336 (2000).